

## Separation and Identification of Functional Groups of Molecules Responsible for Fluorescence of Biodiesel Using FTIR Spectroscopy and Principal Component Analysis

*Humbervânia R. G. da Silva,<sup>a</sup> Cristina M. Quintella\*<sup>a</sup> and Marilena Meira<sup>b</sup>*

<sup>a</sup>Instituto de Química, Universidade Federal da Bahia, Campus Ondina, Rua Barão de Jeremoabo, 40170-290 Salvador-BA, Brazil

<sup>b</sup>Instituto Federal da Bahia, Campus Simões Filho, Av. Universitária, s/n, Pitanguinha, 43700-000 Simões Filho-BA, Brazil

In order to separate and identify functional groups of molecules responsible for fluorescence compounds present in biodiesel, a column chromatography coupled with infrared spectroscopy and multivariate analysis was performed. A biodiesel sample was packed in a chromatographic column and the fractions obtained were used to perform the analyses. Before undergoing the separation process, the biodiesel sample was analyzed by light emitting diode (LED)-induced fluorescence and compared its spectrum with  $\beta$ -carotene and soybean oil patterns. The low cost and speed of analysis suggest that this technique can be used in the separation of biodiesel substances. The fluorescence emission spectra allowed identifying molecules such as  $\beta$ -carotene, in which the spectrum of its pattern exhibited fluorescence within a region ranging from 500 to 700 nm and chlorophyll molecules. When soybean oil is excited at around 405 nm, it features a fluorescent emission band within the region of 670 nm, which reveals the presence of chlorophyll. Infrared spectroscopy coupled with principal component analysis allowed to discriminate the fractions and to identify the functional groups of compounds present in the sample.

**Keywords:** biodiesel, fluorophores, infrared spectroscopy, fluorescence, principal component analysis

### Introduction

Researchers and scientists have begun to evaluate new sources of renewable energy in order to reduce crude oil consumption, since it is classified as a great polluter of the environment. Additionally, due to the increasing cost of barrels of crude oil and the reduction of reserves, interest in biofuels have emerged as alternative clean and renewable energy. Biodiesel is an alternative renewable biofuel of low-toxicity that can be used in diesel engines with or without modification. Currently, biodiesel is being used by several countries as a solution which requires policies for production in order to be used in the transport sector.<sup>1,2</sup>

Biodiesel combustion in engines leads to reduction of smoke, suspended particulates, carbon monoxide (CO) and hydrocarbon emissions (HC). However, it increases emissions of nitrogen oxide (NO<sub>2</sub>), improving or maintaining motor efficiency.<sup>2-5</sup> The kinematic, viscosity, density, and calorific value properties of biodiesel are the

most important parameters that affect engines performance and also emission characteristics. High viscosity of biodiesel is one of the main problems when the fuel is used in diesel engines. In addition, its density is also a very important parameter, because its variation affects the supply and pulverization of the fuel during the injection in the cylinders.<sup>6</sup>

On the other hand, properties such as viscosity, density, calorific value, oxygen content, auto-oxidation, and heating rate, among others, have influence in the engine efficiency. Various additives have been proposed to improve the engine efficiency, such as methanol and ethanol, which improve the viscosity and reduce fuel consumption.<sup>1</sup>

Biodiesel was inserted in the Brazilian energy matrix on January 13, 2005, by law No. 11,097. In compliance with this law, it was necessary to develop analytical methods to quantify the percentage of biodiesel added to diesel fuel. In the present study, we determined the main fluorophores present in biodiesel made from vegetable oils.

Studies have reported that the main fluorophores of biodiesel are the same as those of vegetable oil, such

\*e-mail: cris5000tina@gmail.com

as unsaturated fats, acids, tocopherols, chlorophylls, pheophytins, phenolic compounds, and vitamins A, D and K.<sup>7,8</sup>

The techniques used to analyze biodiesel composition are: gas chromatography (GC); optical methods such as Fourier transform infrared (FTIR) spectroscopy; ultraviolet-visible spectroscopy (UV-Vis), and Raman spectroscopy.<sup>9,10</sup> Meira *et al.*<sup>11</sup> demonstrated that fluorescence spectroscopy coupled with multivariate analysis can be used as an analytical tool to evaluate the oxidative stability of biodiesel and soybean oil in accordance with the conventional Rancimat method.<sup>11</sup> These authors have also identified the adulteration of biodiesel with vegetable oil using fluorescence spectroscopy.<sup>10-12</sup>

Biodiesel is chemically defined as a mixture of mono-alkyl esters of long-chain fatty acids (C16-C18) derived from vegetable oils and animal fats. It is a domestic renewable fuel for diesel engines and meets the standards and specifications provided by the American Society for Testing and Materials (ASTM D 6751). It can also be used as a fuel additive.<sup>13</sup>

Vegetable oils are composed of fatty alcohols, esters, hydrocarbons, tocopherols, phenolic compounds, volatile compounds, glyceridic compounds, phospholipid compounds, and triterpenic acids. These compounds undergo changes when they are subjected to processes such as hydrolysis, esterification, and oxidation. It is important to determine these constituents in order to evaluate the source and the analytical quality. In addition, this determination will allow to know the best extraction method and detecting possible oil adulteration.<sup>14</sup>

Grilo *et al.*<sup>15</sup> determined the concentration of alpha-tocopherol and gamma-tocopherol in vegetable oils in order to know the amount of vitamin E present in alpha-tocopherol and compare it with the nutritional value. Becerra-Herrera *et al.*<sup>16</sup> identified and quantified phenolic compounds, such as alcohols, secoiridoid derivatives, flavonoids, phenolic acids, and aldehydes, present in virgin and extra-virgin olive oil using the dispersive liquid-liquid microextraction combined with ultra-high-pressure liquid chromatography coupled with electrospray ionization-mass spectrometry.<sup>16</sup>

Ballus *et al.*<sup>17</sup> used gas chromatography with flame ionization detection to conduct a quantitative study of tocopherol compounds and phenolic and fatty acids contained in virgin olive oil produced in the southwest region of Brazil.<sup>17</sup> The goals of the present study were to separate the compounds present in biodiesel using column chromatography and infrared spectroscopy in combination with covariant analysis, and determine the wavelengths responsible for this separation in order to

identify functional groups of the molecules responsible for biodiesel fluorescence.

## Experimental

### Materials and methods

#### Biodiesel

The biodiesel sample (B100) was obtained from the Brazilian Petroleum Corporation (PETROBRAS) in Candeias, Bahia State, Brazil, and received it on November 28, 2014. Table 1 shows the test certificate of the sample used. Refined soybean oil was purchased from a local supermarket, which owned the trademark of the product.

#### Patterns

The patterns used were: type 1 synthetic  $\beta$ -carotene (Sigma-Aldrich, St. Louis, Missouri, USA); liquid yellowish-brown  $\alpha$ -tocopherol (99.9% purity, Supelco, Bellefonte, Pennsylvania, USA); and linolenic acid ( $\geq 99\%$  purity, Sigma-Aldrich, St. Louis, Missouri, USA) stored at a temperature range of 0 to  $-20$  °C.

#### Solvents

The solvents used to determine the best eluent using thin-layer chromatography were: acetone, hexane, isopropyl alcohol, *n*-heptane, ethyl alcohol, petroleum ether, ethyl ether, and acetic acid, all with high purity for analysis.

#### Chromatographic analysis

For thin-layer chromatography analysis, 20 × 20 cm aluminium sheets coated with silica gel (DC-Fertigfolie ALUGRAM® Xtra SIL G / UV254) were used. For the separations by column chromatography, it was used the adsorbent silica gel (Sigma-Aldrich, St. Louis, Missouri, USA) with high purity and pore size of 60 Å (63-200  $\mu$ m). The thin-layer chromatography plates were developed using UV light at 254 and 365 nm, and iodine vapour was used as a chemical developer.

#### Experimental procedure

#### Fluorescence spectroscopy

The fluorescent emission spectra of samples were obtained in a light emitting diode (LED) fluorimeter, model Q798FIL (Quimis®, São Paulo, Brazil), equipped with LED lamp, quartz cuvettes, 1 cm optical path, automatic reading of fluorescence spectra of samples with a 0.3 nm resolution, matrix-type silicon photodetector

**Table 1.** Characterization of biodiesel (B100)

Characteristic	Method	Specification	Result
Specific mass at 20 °C / (kg m <sup>-2</sup> )	ASTM D 4052	850 to 900	879.6
Kinematic viscosity at 40 °C / (mm <sup>2</sup> s <sup>-1</sup> )	ASTM D 445	3.0 to 6.0	4.260
Water content / (mg kg <sup>-1</sup> )	ASTM D 6304	200 max	192
Flash point / °C	ASTM D 93	100 min	133
Ester content / % (m/m)	EN 14103	96.5 min	97.6
Total sulfur / (mg kg <sup>-1</sup> )	ASTM D 5453	10 max	3.8
Sodium content + potassium / (mg kg <sup>-1</sup> )	NBR 15556	5 max	1.2
Calcium content + magnesium / (mg kg <sup>-1</sup> )	NBR 15553	5 max	1.6
Phosphorous content / (mg kg <sup>-1</sup> )	NBR 15553	10 max	1.5
Total acidity index / (mg of KOH g <sup>-1</sup> )	ASTM D 664	0.50 max	0.42
Free glycerine / wt.%	ASTM D 6584	0.02 max	0.011
Total glycerine / wt.%	ASTM D 6584	0.25 max	0.185
Monoglycerides content / wt.%	ASTM D 6584	0.7 max	0.615
Diglycerides content / wt.%	ASTM D 6584	0.20 max	0.100
Triglycerides content / wt.%	ASTM D 6584	0.720 max	< 0.050
Iodine index / (g of iodine per 100 g)	EN 14111	–	93
Oxidative stability at 110 °C / h	EN 14112	8 min	11.2
Fatty compounds	40% soy	30% cotton	30% tallow

(2048 points), wavelength range of 350 to 1000 nm, and  $\pm 1.5$  nm accuracy.

To obtain the fluorescence spectra, it was used a fixed excitation wavelength (468-478 nm; blue LED), and signal integration time of 1000 ms. The fluorescent emission spectra of the samples were obtained by exciting them with LED at 468 nm and capturing the emission within the range 488-1000 nm with increments of 1 nm, making a total of 1 excitation wavelength and 615 emission wavelengths. As samples were used without solvent addition, only the beta carotene standard was diluted in hexane.

#### Thin-layer chromatography - determination of the best eluent

Thin-layer chromatography was used to evaluate the best solvent to be used in column chromatography. It was added 1  $\mu$ L of biodiesel on the plate (about 10 cm long) using a capillary tube. The plate was placed in contact with a mixture of solvents. It was performed several tests with different mixtures of solvents, including hexane/acetic acid, petroleum ether/ethyl ether/acetic acid, and petroleum ether/methanol in increasing order of polarity during the time in which the solvent front reached the top of the plate. The plates were placed in contact with iodine vapour that acted as chromogenic reagent. The results showed that the mixture hexane/acetic acid exhibited the best separation.

#### Column chromatography - isolation and purification of chemical constituents of biodiesel

Biodiesel was subjected to column chromatography (silica gel 60). The mixture hexane/acetic acid (9:1) in increasing order of polarity was used as eluent. We collected fractions of approximately 20-25 mL each from this column. They were left to dry at room temperature and then FTIR analyzes were performed. Subsequently, the spectra were analyzed and then the principal component analysis (PCA) was performed to group the samples subfractions.

#### Absorption spectroscopy in the infrared region by Fourier transform infrared spectrometry

The absorption measurements in the infrared region were obtained by FTIR analysis using a spectrophotometer model FT-IR Spectrometer Frontier (PerkinElmer®, São Paulo, Brazil). It was used an attenuated total reflectance (ATR) accessory with a zinc selenide crystal. The measurements were made using 4 cm<sup>-1</sup> resolution, transmission of 4000 to 650 cm<sup>-1</sup>, and 16 scans. The spectra were obtained at room temperature. During the analysis of the samples, it was obtained the absorbance and transmittance data with respect to the wavelengths.

Infrared spectroscopy combined with Fourier transform is one of the most frequently used spectroscopic

techniques for compounds identification. The main advantage of this method is the high sensitivity, rapidity and it is a relatively inexpensive technique. Association of FTIR with PCA provides additional information due to loadings and allows classification of the samples without any chemical analysis.

In this study, FTIR spectra of the subfractions of the sample of biodiesel obtained from the column chromatography were recorded using horizontal ATR as sampling methods. The spectral information constitutes the experimental data which were analyzed by PCA.

PCA is a method for extraction of the systematic variations in one data set and can be used for classification, description and interpretation. The purpose of PCA is to decompose the data matrix and concentrate the source of variability in the data into the first few components. Each principal component represents the main systematic variation in the data set. PCA when applied in FTIR spectra, the data are arranged in a 3D matrix being necessary to transform in 2D matrix. Unfold-PCA is a technique that converts a 3D matrix into a 2D matrix with dimensions  $30 \times 3351$ . Each column of the resulting matrix is mean centered and submitted to PCA to obtain the loadings. After the PCA, the spectra were grouped and interpreted one typical spectrum of each PCA group.

## Results and Discussion

### Fluorescence spectroscopy

Figure 1 shows the fluorescent emission spectra of soybean oil (A), biodiesel (B), and  $\beta$ -carotene pattern (C) at 468 nm excitation. It can be observed maximum emissions of 535 and 670 nm in vegetable oil, and of 535 and 760 nm in biodiesel oil. According to Sikorska *et al.*<sup>8</sup> when soybean oil is excited at around 405 nm, it features a fluorescent emission band around 670 nm, which is attributed to the presence of chlorophyll. Other studies have demonstrated that the main fluorophores of biodiesel are the same as those of vegetable oil.<sup>7,8,18-20</sup> This way, chlorophyll contributes to biodiesel fluorescence between 665 and 675 nm.<sup>12</sup> Magalhães *et al.*<sup>20</sup> detected the presence of chlorophyll in soybean biodiesel when the sample was excited at 532 nm.

The emission spectrum showed that the chlorophyll peak present in biodiesel had more intensity than the spectrum peak of soybean oil. It was also possible to observe that the spectrum of the patterns of  $\beta$ -carotene features fluorescence ranging from 500 to 700 nm. Albuquerque *et al.*<sup>18</sup> characterized Buriti oil and stated that, when the oils go through the transesterification process,

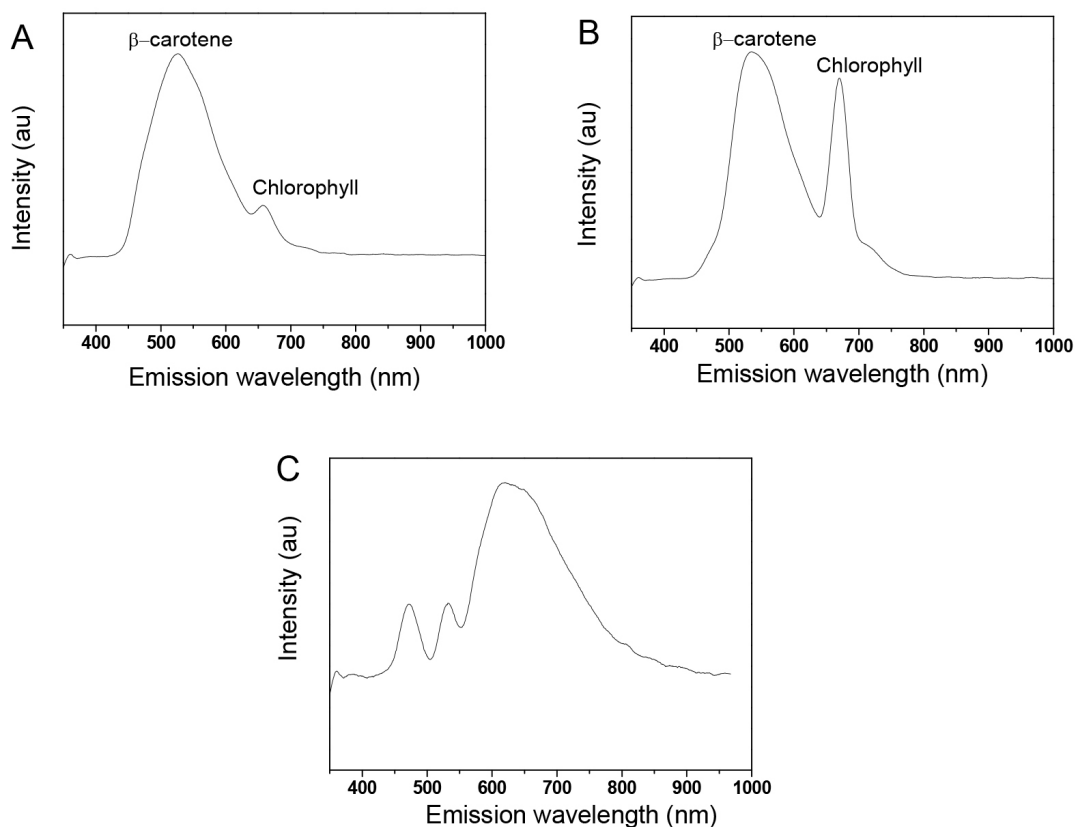


**Figure 1.** Fluorescence emission spectra of soybean oil (A), biodiesel (B), and  $\beta$ -carotene (C) at 468 nm excitation.

they exhibit substances such as  $\beta$ -carotene in their chemical composition. These substances contribute to fluorescence of biodiesel samples (500 to 650 nm) and absorption in the UV-Vis region.<sup>20</sup>

This way, the analyzed biodiesel exhibited carotenoid substances with emission wavelength range of 470 to 620 nm with maximum fluorescence at 530 nm, showing a hypsochromic shift when compared with the maximum absorption of patterns of  $\beta$ -carotene that occurs at approximately 620 nm.

Some works attributed the fluorescence of oil and biodiesel to molecules such methyl esters, tocopherols and carotenoid substances.<sup>18-20</sup> Magalhães *et al.*<sup>20</sup> showed that the methyl linolenate standard, when excited between 280 and 330 nm, emits fluorescence between 350-575 nm and maximum at 410 nm, and  $\alpha$ -tocopherol diluted in *n*-hexane, when excited between 280 and 440 nm, exhibit a fluorescence band between 300 and 400 nm. They attributed the fluorescence of soybean and canola biodiesel to the presence of conjugated tetraenes with two less intense absorption bands at 302 and 316 nm.<sup>20</sup> The sample of biodiesel that was used in this work when excited at 468 nm did not present the characteristic fluorescence band of methyl linoleate in the region of 350-375 nm with

a maximum of 410 nm. The same biodiesel sample when excited at 468 nm also did not present the fluorescence band between 280-440 nm, characteristic of  $\alpha$ -tocopherol.

Sikorska *et al.*<sup>8</sup> attributed the presence of tocopherols and tocotrienols to the emission bands observed in the range 270-300 nm. Poulli *et al.*<sup>21</sup> reported that oleic acid shows a fluorescence band at 405 nm whereas butyric and linoleic acid show fluorescence bands at 273 and 325 nm, respectively. Therefore, oleic acid, butyric and linoleic acid should not contribute to the fluorescence from our biodiesel samples under excitation in the 468 nm range.

Absorption spectroscopy in the infrared region by Fourier transform infrared

Figure 2 shows the FTIR spectra of soybean oil (A), biodiesel (B100) (B), and  $\beta$ -carotene (C). The spectrum of soybean oil showed a triacylglycerol absorption band at 1743  $\text{cm}^{-1}$ . This band was also observed in the soybean biodiesel, but with a shift to 1740  $\text{cm}^{-1}$ , because, when the transesterification reaction occurs, the absorption band of triacylglycerol at 1743  $\text{cm}^{-1}$  is shifted to lower wavenumbers (lower energy) due to the formation of methyl esters of smaller chains than those of starting

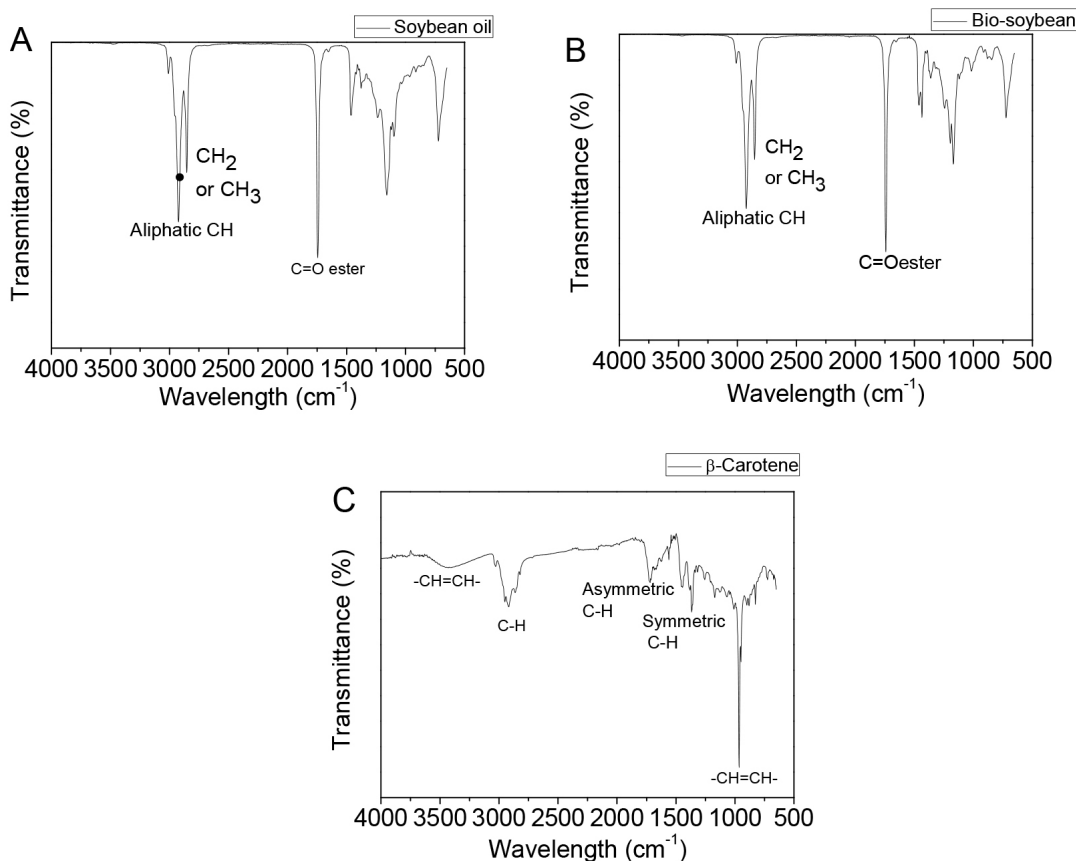


Figure 2. FTIR spectra of soybean oil (A), biodiesel (B), and  $\beta$ -carotene (C).

tri-esters present in oils.<sup>8,18,19</sup> In the spectrum of patterns of  $\beta$ -carotene, the weak absorption band at  $3436\text{ cm}^{-1}$  resulted from  $\beta$ -carotene *trans*-CH=CH bond. The  $2863\text{ cm}^{-1}$  band was due to CH stretching, the  $1623\text{ cm}^{-1}$  band was due to asymmetric deformation, and the  $1337\text{ cm}^{-1}$  band resulted from the symmetric deformation mode of the C–H group. The  $980\text{ cm}^{-1}$  band corresponded to alkene (*trans*-CH=CH) with out-of-plane deformation.

The covariant analysis of the data obtained from the FTIR transmittance spectra is shown in Figure 3. Five PCs were responsible for 99.88% of the variance, being 91.71% of the variance for PC1, 5.03% for PC2, 2.51% for PC3, 0.46% for PC4 and 0.17% for PC5. The PC3 component and the further ones contribute less than 3% of the residual variance. Being so, we can assume that these PCs model non-significant variations, such as noise or sampling variations.

The first principal component explains 99.71% of the data set variance and represents the most dominant information. So, the scores associated with PC1 reveal that

the extracted spectral features are highly correlated with chemical structure.

The scatter plot of PC1 against PC2 (Figure 3) shows formation of 4 groups separated according to chemical similarity of the samples. Fractions 1, 2 and 3 were found in the region of negative PC1 and negative PC2, fraction 4 to 20 and 22 in the region of negative PC1 and positive PC2, and sample 4 appeared in the region of negative PC2, fractions 21 and 23 in the region of positive PC1 and positive PC2.

The last fractions that were collected from the chromatographic column were in the region of positive PC1 and negative PC2, except sample 28 lying in the region of positive PC2. From the loadings spectra (Figure 4) it was possible to identify the wavelengths responsible for this separation and to relate the loadings with the spectra obtained from the FTIR analysis (Figure 5) to determine the types of chemical bonds that contributed to such a grouping.

Figure 3 shows the PCA with the PC1 scores with respect to the PC2 scores in the biodiesel fractions obtained

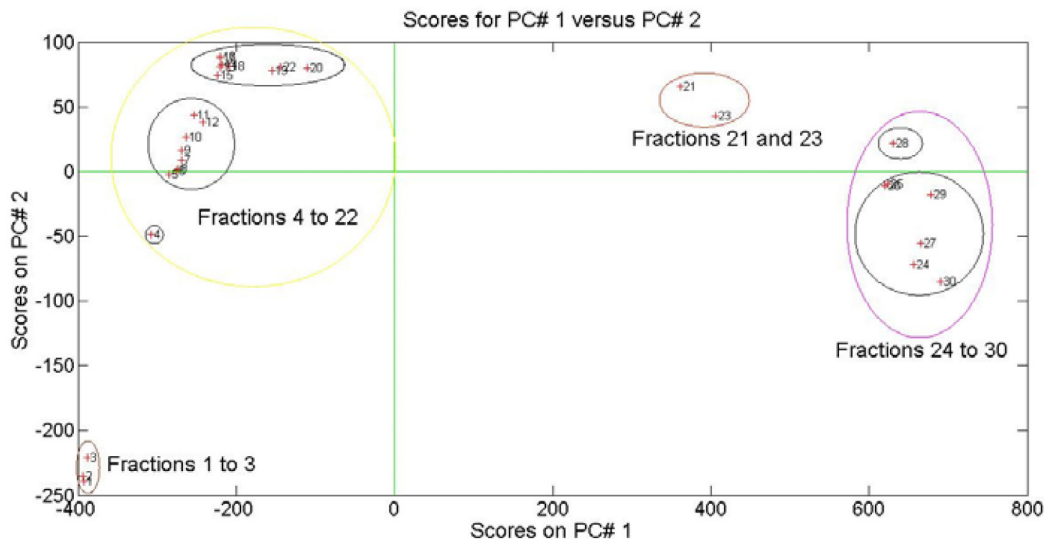


**Figure 3.** Principal component analysis of the fractions obtained by chromatography of biodiesel.

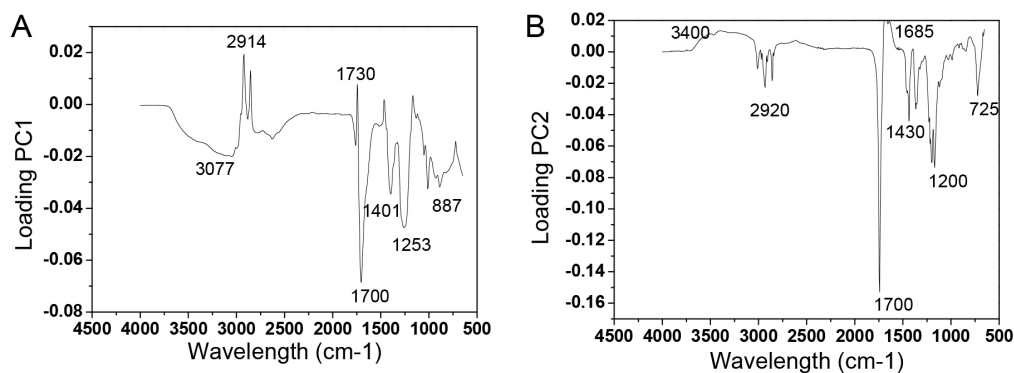


**Figure 4.** PC1 (A) and PC2 (B) loadings with respect to the number of variables in the PCA for fractions 1 to 30.

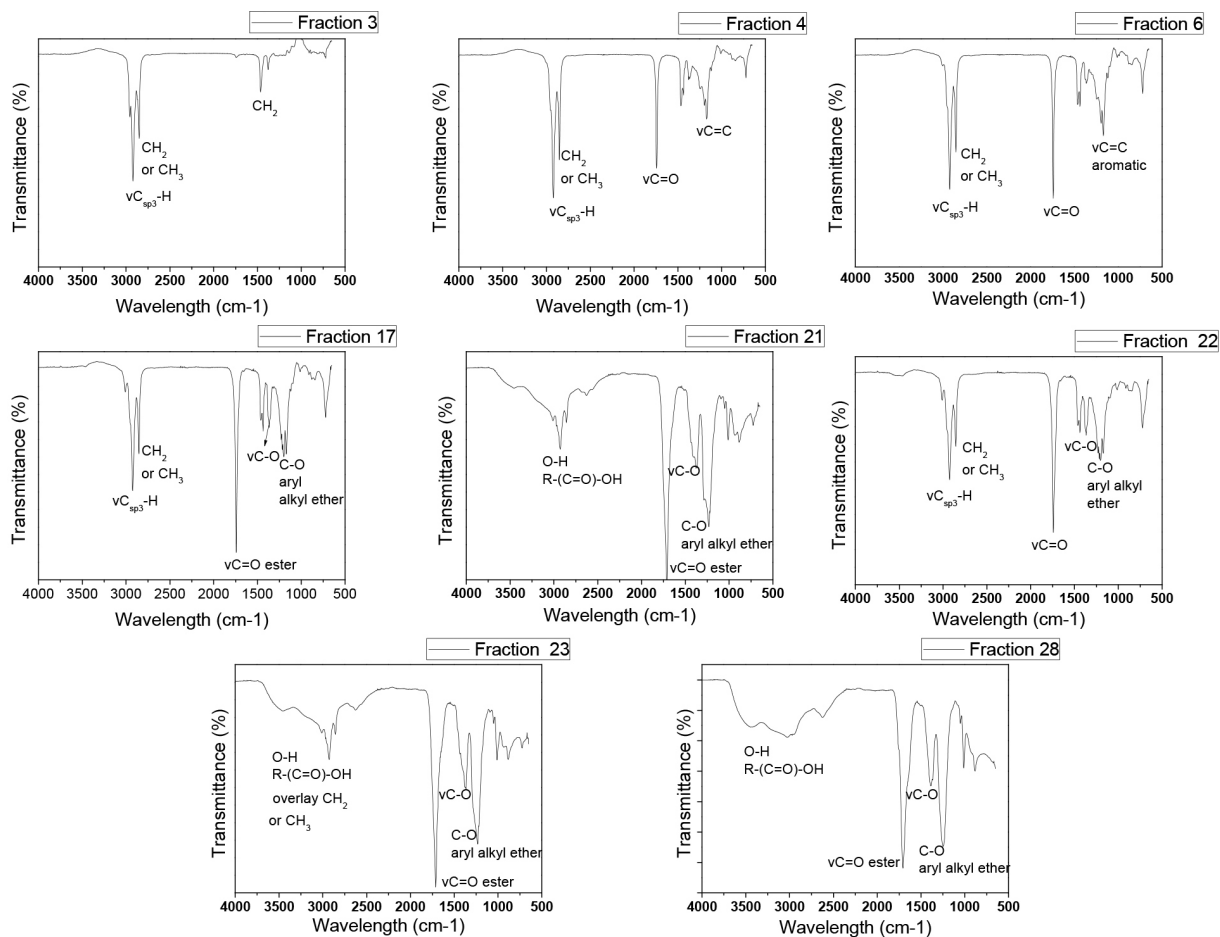


**Figure 5.** Fourier transform infrared spectroscopy of a fraction that represents each group formed by the principal component analysis.

by column chromatography. The PCA resulted in the separation of four different groups. Figure 4 shows PC1 (A) and PC2 (B) loadings with respect to the wavelengths for the PCA with the 30 samples.

The separation by PCA (Figure 3) associated with the loadings (Figure 4), and the spectra obtained by FTIR analysis (Figure 5) explain the separation that occurred in the PCA and identify the functional group responsible for this separation taking into consideration the wavelengths. It is possible to observe the groups of spectra in the same quadrant due to the similarity of the functional groups, and dispersion of some samples due to the difference in absorption intensity.

The first three fractions were grouped in the third quadrant, a region where PC1 and PC2 were negative. The most influential loadings in this separation were 3077 and 1401  $\text{cm}^{-1}$  for PC1, and 2920 and 1430  $\text{cm}^{-1}$  for PC2. It is possible to affirm that these samples were separated from the others due to the intensity of the peaks of  $\text{CH}_2/\text{CH}_3$  deformation, and the absence of the  $\text{C}=\text{O}$  bond in this group of spectra, showing only bonds of hydrocarbon groups.

Fraction 4 (Figure 3) appeared in the third quadrant and fractions 5 to 20 in the second quadrant. The FTIR spectrum of fraction 4 (Figure 5) was similar to the spectra of fractions 5 to 20. As a result, they should have been in the same region, but they were differentiated by the intensity of the peaks. The peaks of fraction 4 had a lower absorption intensity than the peaks of the other fractions. The fractions of the second quadrant were in a region where the PC1 was negative and the PC2 positive. The loadings chart (Figures 4A and 4B) and the FTIR spectra (Figure 5) allow to affirm that the wavelength that influenced the separation of this group from the others was 1700  $\text{cm}^{-1}$  for PC1 and PC2, which represents the  $\text{C}=\text{O}$  stretching. Within that group, it is possible to observe two other groups formed by fractions 5 to 12 and 13 to 20. These two groups were also differentiated by the intensities of the transmittance peaks, which were more intense in fractions 13 to 20.

Fraction 22 appeared in the second quadrant separated from the group of fractions 21 and 23, even though its FTIR spectrum (Figure 5) was similar to the spectra of those two fractions. That spectrum of fraction 22 showed  $\text{C}-\text{O}$  bonds at 1400 and 1200  $\text{cm}^{-1}$ , region of negative PC1

and positive PC2. The fact that it was out of this region can be explained by the possible occurrence of some contamination during the process of solvent evaporation after column chromatography, because the sample was opened for a few days.

Fractions 21 and 23 were in the first quadrant, region of positive PC1 and PC2. The spectra of these two samples were similar and there was a slight difference in the intensity of absorption peaks. The transmittance peaks of these samples were in the region of  $3300\text{ cm}^{-1}$  (positive PC2 loading), indicating the presence of O–H of free carboxylic acids. Fatty acids are carboxylic acids with a R–(C=O)–OH structure, showing characteristic absorption of OH groups around  $3300$  and  $2500\text{ cm}^{-1}$ , and  $1730\text{ cm}^{-1}$  (positive PC1 loading) indicates the presence of C=O of ester grouping. These samples showed absorption peaks of  $\text{CH}_2/\text{CH}_3$  groups around  $2900\text{ cm}^{-1}$  (positive PC1 loading) overlapping the O–H band. The presence of these overlapped groups separated them from the samples of the fourth quadrant.

Fractions 24 to 30 were in the fourth quadrant, where PC1 was positive and PC2 negative. This group of samples exhibited absorption peaks at  $3400\text{ cm}^{-1}$  (negative PC2 loading), indicating the presence of O–H stretching. The peak was very intense at  $1730\text{ cm}^{-1}$  (positive PC1 and negative PC2 loadings), indicating the presence of C=O, peak at  $1430$  and  $1200\text{ cm}^{-1}$  (negative PC2 loading), which can be attributed to the presence of geminal  $\text{CH}_3$  and peak at  $1000\text{ cm}^{-1}$ , confirming the presence of O–H out-of-plane (negative PC2 loading). The sample 28 appeared in a region of the first quadrant, a little above the region of the group

with similar spectra (Figure 5); however, it was different from the other samples due to the intensity of the peaks  $3400\text{ cm}^{-1}$  (positive PC2 loading),  $1730$  and  $1685\text{ cm}^{-1}$  (positive PC1 and positive PC2 loading) of the groups O–H and C=O.

The PCA was remade removing the sample 22 in order to make a comparison with the PCA of Figure 3. It was possible to observe that, according to the PCA chart and the charts that represent the loadings, there was no change in the separation of the sample groups. This implies that, even though the sample 22 appeared in a region where its spectrum differed from the others, there was no change in the separation by PCA.

The covariant analysis of the data in combination with spectroscopy allowed grouping similar samples after their separation by column chromatography. It also led to the possibility to observe the separation of four possible different compounds.

The covariant analysis of the data obtained from the FTIR absorbance spectra without the sample 22 is shown in Figure 6. The best separation of groups occurred in PC1 as a function of PC3. It was possible to observe that the PCA groups obtained are the same obtained with the transmittance data, showing that the methodology is not influencing the separation of groups. The only change is on the relevant PCA axis combination: PC1 *versus* PC2 for transmittance and PC1 *versus* PC3 for absorbance.

In this work, our aim was to separate the groups, thus both absorbance and transmittance may be used, as they have yield the same groups, although the regions where

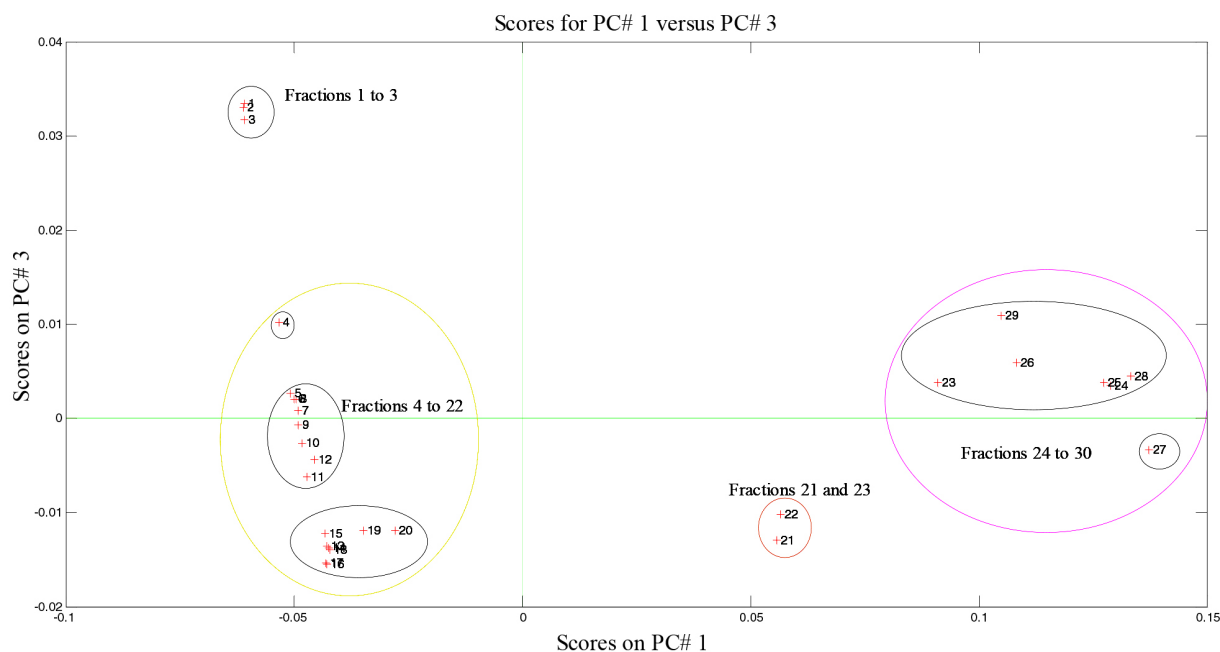


**Figure 6.** Principal-component analysis of the fractions obtained by chromatography of biodiesel from the FTIR absorbance spectra.

they are in the scores graphic are different. Nevertheless, considering that the transmittance model explains 96.74% of the variance (adding the PC1 and the PC2 variances), and the absorbance model explains 95.35% of the variance (adding the PC1 and the PC3 variances), the better resolution will be attained by the transmittance model.

## Conclusions

The emission spectra of molecular fluorescence allowed identifying molecules such as  $\beta$ -carotene and chlorophyll, both in soybean oil and soybean biodiesel. The separation by column chromatography, followed by infrared spectroscopy analysis in combination with PCA allowed discriminating the fractions by functional groups separation. It was also possible to determine the chemical groups responsible for this separation, namely:  $\text{CH}_2/\text{CH}_3$  and  $\text{C}=\text{O}$  of carboxylic acid in the positive PC1; and  $\text{C}=\text{O}$  of ester and  $\text{C}-\text{O}$  bond in the negative PC1.  $\text{O}-\text{H}$  and  $\text{C}-\text{O}$  stretching separated the samples in the region of positive PC2, and  $\text{CH}_2/\text{CH}_3$  deformation,  $\text{C}=\text{O}$  of ester, and geminal  $\text{CH}_3$ , in the region of positive PC2.

## Supplementary Information

Supplementary information (other FTIR graphics) is available free of charge at <http://jbcs.org.br> as PDF file.

## Acknowledgments

This work was supported by the National Institutes of Health National Counsel of Technological and Scientific Development and Fundação de Amparo à Pesquisa do Estado da Bahia.

## References

1. Shaahir, V. K.; Jawahar, C. P.; Suresh, P. R.; *Renewable Sustainable Energy Rev.* **2015**, *45*, 686.
2. Quintella, C. M.; Teixeira, L. S.; Korn, M. G.; Costa Neto, P. R.; Torres, E. A.; Castro, M. P.; Jesus, C. A.; *Quim. Nova* **2009**, *32*, 793.
3. Nabi, M. N.; Rahman, M. N.; Akhter, M. S.; *Appl. Therm. Eng.* **2009**, *29*, 2265.
4. Qi, D. H.; Geng, L. M.; Chen, H.; Bian, Y. Z. H.; Liu, J.; Ren, X. C. H.; *Renewable Energy* **2009**, *34*, 2706.
5. Aydin, H.; Ilkilic, C.; *Appl. Therm. Eng.* **2010**, *30*, 1199.
6. Alptekin, E.; Canakci, M.; *Renewable Energy* **2008**, *33*, 2623.
7. Dupuy, N.; Le Dréau, Y.; Ollivier, D.; Artaud, J.; Pinatel, C.; Kister, J.; *J. Agric. Food Chem.* **2005**, *53*, 9361.
8. Sikorska, E.; Gliszczynska-Swkgiglo, A.; Khmelinskii, I.; Sikorski, M.; *J. Agric. Food Chem.* **2005**, *53*, 6988.
9. Reda, S. Y.; Carneiro, P. B.; *Rev. Cienc. Agron.* **2009**, *40*, 48.
10. Meira, M.; Quintella, C. M.; Ferrer, T. M.; Gonçalves, H. R.; Guimaraes, A. K.; Costa Neto, P. R.; Pepe, I. M.; *Quim. Nova* **2011**, *34*, 621.
11. Meira, M.; Quintella, C. M.; Tanajura, A. S.; Silva, H. R. G.; Fernando, J. D. S.; Costa Neto, P. R.; *Talanta* **2011**, *85*, 430.
12. Tomazzoni, G.; Meira, M.; Quintella, C. M.; Zaagonel, G. F.; Costa, B. J.; Oliveira, P. R.; Pepe, I. M.; Costa Neto, P. R.; *J. Am. Oil Chem. Soc.* **2013**, *91*, 215.
13. World Customs Organization; [http://www3.wcoomd.org/home\\_hsoverviewboxes\\_tools\\_and\\_instruments\\_hsconvention.htm](http://www3.wcoomd.org/home_hsoverviewboxes_tools_and_instruments_hsconvention.htm), accessed in May 2017.
14. Moreda, W.; Cert, A.; Pérez-Camino, A. C.; *J. Chromatogr. A* **2000**, *881*, 131.
15. Grilo, E. C.; Costa, P. N.; Sanzio, G. C. S.; Beserra, A. F. L.; Almeida, F. N. S.; Dimenstein, R.; *Food Sci. Technol.* **2014**, *34*, 379.
16. Becerra-Herrera, M.; Sanchez-Astudillo, M.; Beltran, R.; Sayago, A.; *Food Sci. Technol.* **2014**, *57*, 49.
17. Ballus, C. A.; Meinhart, A. D.; Campos Jr., F. A. S.; da Silva, L. F. O.; Oliveira, A. F.; Godoy, H. T.; *Food Res. Int.* **2014**, *62*, 74.
18. Albuquerque, M. L. S.; Guedes, I.; Alcantara, J. P.; Moreira, S. G. C.; Neto, N. M. B.; Correa, D. S.; *J. Braz. Chem. Soc.* **2005**, *16*, 1113.
19. Meira, M.; Quintella, C. M.; Pepe, I. M.; Costa Neto, P. R.; Ribeiro, E. M. O.; Del Cid, A. L.; Guimaraes, A. K.; *Spectrochim. Acta, Part A* **2014**, *1*, 1.
20. Magalhães, K. F.; Caires, A. R. L.; Silva, M. S.; Alcantara, G. B.; Oliveira, S. L.; *Fuel* **2014**, *119*, 120.
21. Poulli, K. I.; Mousdis, G. A.; Georgiou, C. A.; *Anal. Chim. Acta* **2005**, *542*, 151.

Submitted: February 24, 2017

Published online: May 18, 2017